Strong-coupling theory of electronic Raman scattering in high-temperature superconductors

T. Dahm
Max-Planck-Institut für Physik komplexer Systeme, Nöthnitzer Straße 38, D-01187 Dresden, Germany

D. Manske* and L. Tewordt
I. Institut für Theoretische Physik, Universität Hamburg, Jungiusstraße 9, D-20355 Hamburg, Germany

(Received 20 May 1998; revised manuscript received 25 January 1999)

We have calculated the response function for electronic Raman scattering within the fluctuation-exchange approximation for the two-dimensional Hubbard model. Below T_c, a large pair-breaking peak and a gap develop in the B_{1g} spectrum while the effect of superconductivity on the B_{2g} spectrum is much smaller. In order to investigate the underdoped regime we study the influence of a phenomenologically introduced pseudogap. In the normal state we find that this pseudogap leads for decreasing temperature to development of a d-wave gap structure in the density of states which merges continuously into the superconducting spectrum. A corresponding pair-breaking peak evolves continuously in the B_{1g} Raman spectrum as T decreases in the normal state and below T_c. We discuss our results in connection with recent tunneling, optical conductivity, and Raman data on the cuprates. [S0163-1829(99)13721-4]

I. INTRODUCTION

Electronic Raman scattering is an important tool to investigate the symmetry of the order parameter in the high-T_c superconductors. Raman scattering data below T_c on optimally doped $Bi_2Sr_2CaCu_2O_{8+\delta}$ (Bi2212) for the different polarization channels of A_{1g}, B_{1g}, and B_{2g} symmetry have been analyzed by weak-coupling BCS theory and found to be in agreement with $d_{x^2-y^2}$ pairing symmetry.[1] In the weak-coupling limit it has been shown that good agreement with the $A^{x'x'}$ and B_{1g} Raman data on $YBa_2Cu_3O_7$ (YBCO) can be obtained if vertex corrections due to the pairing interaction and short-range Hubbard-type interactions between the electrons are taken into account.[2] The relationship between the normal-state anomalous Raman spectrum and the optical conductivity of high-T_c superconductors has been discussed in the context of marginal Fermi liquid (MFL) theory where it has been noted that a linear frequency variation of the quasiparticle damping is responsible for these phenomena.[3] This is consistent with the results of the nested Fermi liquid (NFL) model which describes the qualitative features of the optical conductivity and Raman response in the normal state correctly and can be generalized in a simple way to the superconducting state.[4] Strong-coupling calculations with anisotropic Eliashberg equations have been carried out by using a phenomenological anisotropic spin fluctuation interaction for a nearly antiferromagnetic Fermi liquid (NAFL) theory.[5] These theories are capable of explaining many features of the observed Raman spectra in $La_{2-x}Sr_xCuO_4$,[6] Bi2212,[7] and YBCO.[8] In the latter work it is shown that the Raman response is extremely sensitive to the details of the band structure and the anisotropy of the spin fluctuation interaction. Comparison of the low frequency B_{1g} and B_{2g} response in the normal state could provide an indication of the strength and anisotropy of the interaction. The pair breaking peak in the B_{1g} response carries information on quasiparticle scattering.

In this paper we present results for electronic Raman scattering in the layered cuprates which are based on the fluctuation-exchange (FLEX) approximation[9] for the spin and quasiparticle excitations in the two-dimensional (2D) one-band Hubbard model.[10] The FLEX approximation is a self-consistent and conserving approximation scheme in the sense of Kadanoff and Baym[11] and goes well beyond mean-field approximation. Especially the feed-back effect of the one-particle properties on the spin fluctuation spectrum is taken into account self-consistently and has important consequences in particular in the superconducting state. For example, the quasiparticle damping which varies linearly with frequency in the normal state in accordance with MFL (Ref. 3) and NFL (Ref. 4) theories, is strongly suppressed at lower frequencies in the superconducting state. These properties of the quasiparticle damping determine to a large extent the optical conductivity and Raman spectra in the normal and superconducting states. The FLEX approximation has been shown to yield a number of unusual phenomena, which also have been observed in the high-T_c cuprates, as, for example, a dip feature in the photoemission spectra, a resonance in the neutron scattering intensity and a rapid opening of the gap below T_c.[10,13,14] Therefore it is worthwhile to apply this approximation scheme to the electronic Raman scattering intensity and compare the results with the experiments. Using this approximation scheme goes beyond previous theories of electronic Raman scattering,[1,2,6–8] where either the gap in the superconducting state or the spin fluctuation interaction in the normal state were taken as phenomenological functions. In the strong-coupling calculations[6,8] the same model interaction is used in the Eliashberg equations for the self-energy as well as the superconducting gap. We shall see that the neglection of the feed-back effect of the gap on the interaction leads to substantially different results for the Raman response in comparison to those of our self-consistent theory.

In order to make comparison with experiments in the underdoped cuprates it is necessary to take into account the presence of a normal-state pseudogap. It has been shown

previously that such a pseudogap having d-wave symmetry is capable of describing a number of different experiments in underdoped cuprates such as the specific heat and Knight shift,[15] nuclear-spin relaxation rate, angle-resolved photoemission spectroscopy (ARPES),[16] and tunneling density of states.[17] Interpretations of the pseudogap and normal-state properties are manifold (see, e.g., Ref. 15), including d-wave pairing fluctuations[18] and a charge-density-wave (CDW) state.[19] It has been shown that the NMR Knight shift and the thermodynamic data can be modeled by writing the square of the total gap function as the sum of the squares of the d-wave superconducting gap (SC) and the normal-state pseudogap $E_g(\mathbf{k})$ with d-wave symmetry.[15] Such a relationship holds, for example, at the hot spots of the Fermi surface where the nesting condition is satisfied for the SC and CDW gaps.[19] Since we have no firm prescription for calculating this pseudogap from first principles we take here a phenomenological normal state d-wave gap while the additional gap occurring in the superconducting state is calculated self-consistently. It should be pointed out that the effect of the pseudogap on the quasiparticle self-energy and lifetime is taken into account correctly by including it in the Green's functions and spin fluctuation interaction of the FLEX equations. As we will show below, the pseudogap leads to a strong suppression and a gap at low temperatures of the frequency-dependent scattering rate while the scattering rate exhibits a linear frequency variation in the absence of a pseudogap. Furthermore, the effective mass ratio acquires a maximum at about that frequency where the scattering rate rises steeply. The in-plane optical conductivity has the form of a Drude peak whose maximum increases and whose spectral weight at higher frequencies is suppressed for increasing pseudogap amplitude E_g. These results are in qualitative agreement with the infrared response data on underdoped Bi2212, YBCO, and LSCO compounds.[20] We shall see that the (temperature independent) pseudogap leads to the development of a peak in the B_{1g} Raman spectrum for decreasing temperature which has similarities with the observed B_{1g} Raman resonance in the normal state of underdoped Bi2212 compounds.[21]

In Sec. II and in the Appendix A we develop the general theory of the Raman response function within the FLEX approximation. In Sec. III we present and discuss our results. Section IV contains the conclusions.

II. GENERAL THEORY OF THE RAMAN RESPONSE FOR THE 2D HUBBARD MODEL OF d-WAVE SUPERCONDUCTORS

The main equations of the general theory are given in Appendix A. The basis of the FLEX approximation are the generalized Eliashberg equations of the 2D Hubbard model for the quasiparticle self-energy components $\omega[1-Z(\mathbf{k},\omega)]$ and $\xi(\mathbf{k},\omega)$ and the d-wave gap function $\phi(\mathbf{k},\omega)$. These equations are presented in Eq. (A4) in Nambu's 2×2 matrix formalism in terms of Pauli matrices τ_i $(i=0,1,2,3)$ for the self-energy Σ and the Green's function G. The spin and charge fluctuation interactions P_s and P_c are given in terms of the dynamical spin and charge susceptibilities $\chi_s=\chi_{s0}(1-U\chi_{s0})^{-1}$ and $\chi_c=\chi_{c0}(1+U\chi_{c0})^{-1}$ [see Eq. (A4)] where the irreducible susceptibilities $\chi_{s0}(\mathbf{q},\omega)$ and $\chi_{c0}(\mathbf{q},\omega)$ are calculated from the dressed Green's function G given by the Dyson equation in 2×2 matrix form [see Eq. (A3)].

It is instructive to start with the gauge invariant theory for the current-charge correlation function $P_{\mu\nu}$ defined in Eq. (A1).[23] The corresponding vertex function Γ_μ obtained by the ladder approximation with interactions $\tau_0 P_s \tau_0$ and $\tau_3 P_c \tau_3$ is given in Eq. (A5). One can show with the help of the Eliashberg equations [see Eq. (A4)] that Γ_μ satisfies Ward's identity [see Eq. (A6)] to comply with the requirement of gauge invariance.[23] It should be pointed out that the equation for the vertex function Γ_0 of the charge susceptibility agrees with the vertex equation for the irreducible charge susceptibility χ_{c0} which has been derived previously in the framework of a self-consistent and conserving approximation [see Eq. (6) in Ref. 12].

In analogy to the expression for the charge density, $P_{00}=e^2\chi_{c0}$, we obtain the expression for the Raman response function χ_γ by replacing γ_0 and Γ_0 in Eq. (A1) by the bare and full Raman vertices γ and Γ [see Eq. (A8)]. Analytic continuation from imaginary to real frequencies leads to the following expression for the Raman response function:

$$\mathrm{Im}\,\chi_\gamma(\mathbf{q}=0,\omega)=\pi\int_{-\infty}^{\infty}d\omega'[f(\omega')-f(\omega'+\omega)]\times\sum_{\mathbf{k}}\Gamma(\mathbf{k},\omega',\omega)[N(\mathbf{k},\omega'+\omega)N(\mathbf{k},\omega')-A_1(\mathbf{k},\omega'+\omega)A_1(\mathbf{k},\omega')]\gamma(\mathbf{k}). \quad (1)$$

Here, $N(\mathbf{k},\omega)=A_0(\mathbf{k},\omega)+A_3(\mathbf{k},\omega)$ and $A_1(\mathbf{k},\omega)$ are the spectral densities of the Green's functions G and F.[10] The bare Raman vertices for the different polarization symmetries B_{1g}, B_{2g}, and A_{1g} are the following[2]:

$$\gamma_{B_{1g}}=t[\cos(k_x)-\cos(k_y)],$$

$$\gamma_{B_{2g}}=4tB\sin(k_x)\sin(k_y),$$

$$\gamma_{A_{1g}}=t[\cos(k_x)+\cos(k_y)-4B\cos(k_x)\cos(k_y)]. \quad (2)$$

Here, t is the nearest neighbor and $t'=-Bt$ (with $B=0.45$) is the next-nearest neighbor hopping energy in the tight-binding band.[2] It should be pointed out that we have subtracted from the vertex for $A^{x'x'}$ symmetry given in Ref. 2 the vertex for B_{2g} symmetry in order to obtain an A_{1g} component which is fully symmetric with respect to the D_{4h} point group. In the Appendix A we develop the theory of the vertex function for the current-current correlation function and show with the help of the generalized Eliashberg equations [see Eq. (A4)] that it satisfies Ward's identity [see Eq. (A6)]. In analogy we obtain the equations for the Raman response function [see Eq. (A8)] and for the full Raman Vertex [see Eq. (A9)]. The equation for the full Raman vertex Γ is obtained from the equation for the vertex function Γ_0 of the irreducible charge susceptibility χ_{c0} [see Eq. (A5)] by replacing γ_0 by the bare Raman vertex γ. This yields the equation for the full vertex function Γ in Eq. (A9). For the analytic continuation of this equation from imaginary to real frequencies we have to introduce the double-spectral repre-

sentation for the vertex function.[12] In this way we obtain approximately the following integral equation for the vertex function $\Gamma(\mathbf{k},\omega',\omega)$ occurring in Eq. (1):

$$\Gamma(\mathbf{k},\omega',\omega)=\gamma(\mathbf{k})+\pi^2\sum_{\mathbf{q}}\int_{-\infty}^{\infty}d\nu P_s(\mathbf{q},\nu)[f(\nu-\omega'-\omega)+b(\nu)][N(\mathbf{k}+\mathbf{q},\omega'-\nu+\omega)N(\mathbf{k}+\mathbf{q},\omega'-\nu)-A_1(\mathbf{k}+\mathbf{q},\omega'-\nu+\omega)A_1\times(\mathbf{k}+\mathbf{q},\omega'-\nu)]\Gamma(\mathbf{k}+\mathbf{q},\omega'-\nu,\omega). \quad (3)$$

Here, $P_s(\mathbf{q},\nu)=(3/2)U^2\,\mathrm{Im}\,\chi_s(\mathbf{q},\nu)$ is the pairing interaction due to exchange of spin fluctuations (we have left out the interaction due to charge fluctuations because this is much smaller). We now approximate this vertex equation in the following way: first, we consider only the lowest order term by inserting on the right hand side the bare vertex $\gamma(\mathbf{k}+\mathbf{q})$, secondly, we replace $\gamma(\mathbf{k}+\mathbf{q})$ by $\gamma(\mathbf{k}+\mathbf{Q})$ with $\mathbf{Q}=(\pi,\pi)$ because $P_s(\mathbf{q},\nu)$ is strongly peaked at $\mathbf{Q}$ and the equivalent vectors $(\pm\pi,\pm\pi)$. In this way we obtain approximately the following vertex corrections for the three different symmetries of interest:

$$\Gamma_{B_{1g}}(\mathbf{k},\omega',\omega)=t[\cos(k_x)-\cos(k_y)][1-J(\mathbf{k},\omega',\omega)],$$

$$\Gamma_{B_{2g}}(\mathbf{k},\omega',\omega)=4tB\sin(k_x)\sin(k_y)[1+J(\mathbf{k},\omega',\omega)], \quad (4)$$

$$\Gamma_{A_{1g}}(\mathbf{k},\omega',\omega)=t[\cos(k_x)+\cos(k_y)][1-J(\mathbf{k},\omega',\omega)]-4tB\cos(k_x)\cos(k_y)[1+J(\mathbf{k},\omega',\omega)]$$

with

$$J(\mathbf{k},\omega',\omega)=\pi^2\int_{-\infty}^{\infty}d\nu[f(\nu-\omega'-\omega)+b(\nu)]\sum_{\mathbf{q}}P_s(\mathbf{q},\nu)\times[N(\mathbf{k}+\mathbf{q},\omega'+\omega-\nu)N(\mathbf{k}+\mathbf{q},\omega'-\nu)-A_1(\mathbf{k}+\mathbf{q},\omega'+\omega-\nu)A_1(\mathbf{k}+\mathbf{q},\omega'-\nu)]. \quad (5)$$

The functions f and b in Eqs. (3) and (5) are the Fermi and Bose functions. Another estimate of the full vertex function $\Gamma_{B_{2g}}$ is obtained in Appendix A by showing that it is approximately equal to $\gamma_{B_{2g}}\Gamma_0$ where Γ_0 is the vertex function of the charge susceptibility. Making use of the Ward identity for Γ_0 in Eq. (A7) we find that roughly $\Gamma_{B_{2g}}\simeq\gamma_{B_{2g}}Z(\mathbf{k},\omega)$ [more exactly, see result in Eq. (A11)]. This means that the vertex correction for $\Gamma_{B_{2g}}$ corresponding to J in Eq. (4) is of the order $[Z(\mathbf{k},\omega)-1]$. The latter quantity is about 0.8 for $\mathbf{k}$ along the node of the gap and about 1.3 for $\mathbf{k}$ along the antinode of the gap.[14]

III. RESULTS FOR THE RAMAN RESPONSE IN *d*-WAVE SUPERCONDUCTORS

We have solved the FLEX equations [see Eq. (A4)] for a 2D tight-binding band

$$\epsilon(\mathbf{k})=t[-2\cos(k_x)-2\cos(k_y)+4B\cos(k_x)\cos(k_y)-\mu] \quad (6)$$

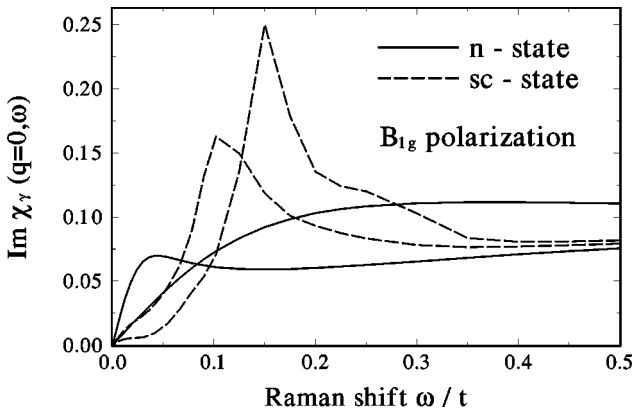

FIG. 1. Raman spectra $\mathrm{Im}\,\chi_\gamma(\mathbf{q}=0,\omega)$ for B_{1g} polarization in the normal state at $T=0.1t$ and $0.023t$ (solid lines with increasing slopes), and in the superconducting state ($T_c=0.022t$) at $T=0.021t$ and $0.017t$, or $T/T_c=0.77$ (dashed lines with increasing peaks).

with $B=0.45$ and $\mu=-1.1$. This describes approximately the Fermi surfaces of Bi2212 and YBCO compounds. Furthermore we take an effective Coulomb repulsion $U(\mathbf{q})$ which has a maximum value $U=3.6$ at $\mathbf{q}=\mathbf{Q}$ and decreases monotonically with decreasing $\mathbf{q}$ to a value $U(0)=0.62$ at $\mathbf{q}=0$. This functional form approximates the calculated vertex corrections to χ_{s0} [see Eq. (8) in Ref. 13]. For a chemical potential $\mu=-1.1$ we obtain a renormalized band filling $n=0.90$ and a superconducting transition at $T_c=0.022t$. We remark that the vertex corrections for the irreducible spin susceptibility $\chi_{s0}(\mathbf{q},\omega)$ is similar to that in Eq. (5) apart from the opposite sign and the dependence on $\mathbf{q}$.[12] We have calculated this vertex correction in Ref. 13. It turns out that the frequency and temperature dependencies are rather weak and that the $\mathbf{q}$ dispersion around $\mathbf{Q}$ can be well approximated by the phenomenological spin-spin coupling which has been used to describe the NMR data for YBCO compounds.[5] Regarding our choice of parameter values we remark that FLEX calculations have been carried out for a large number of parameters $t'=-Bt,\mu,U$, and the constants fitting the $\mathbf{q}$ dispersion of the vertex correction for the susceptibility. The results are qualitatively similar to the present ones apart from the fact that $\mathrm{Im}\,\chi_s(\mathbf{q},\omega)$ as a function of $\mathbf{q}$ exhibits below T_c one broad peak centered at $\mathbf{Q}$ for the next-nearest neighbor hopping $t'=-Bt$ ($B=0.45$) while it exhibits four distinct peaks around $\mathbf{Q}$ for $t'=0$.[10,14]

First we present our results for the Raman response function in Eq. (1) in the absence of vertex corrections to the bare Raman vertices in Eq. (2) [$J=0$ in Eq. (4)]. One sees from Figs. 1 and 2 for B_{1g} and B_{2g} symmetry that in the normal state (solid curves) both spectra start linearly in frequency ω and become flat at high frequencies. The slope at $\omega=0$ increases with decreasing temperature T while the spectrum at high frequencies decreases with decreasing T. In the B_{2g} spectrum a low-frequency peak develops for decreasing T. These results are similar to the normal-state results which have been obtained from the theory of nearly antiferromagnetic Fermi liquids in the $z=1$ pseudoscaling and the $z=2$ mean field scaling regimes.[7] Experimental data available at present do not show a peak in the normal-state B_{2g} response. It has been pointed out that observation of this structure in

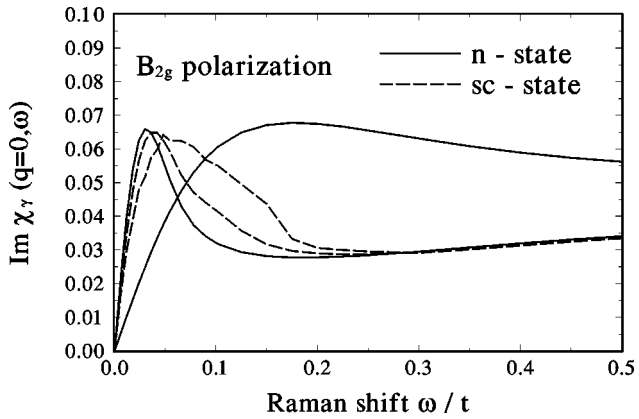

FIG. 2. Raman response function for the B_{2g} channel for the same temperatures as in Fig. 1. In the superconducting state the slope at $\omega=0$ decreases for decreasing T.

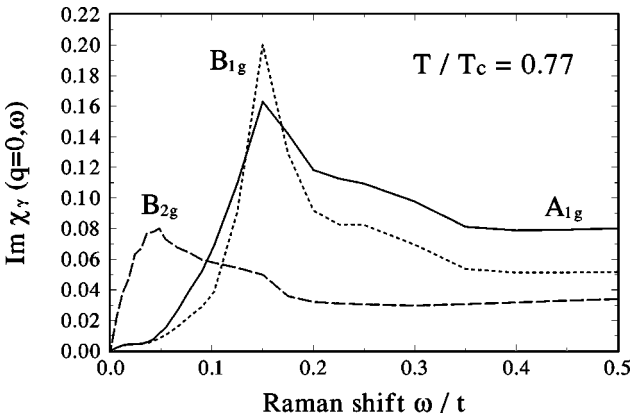

FIG. 3. Raman spectra Im $\chi_\gamma(\mathbf{q}=0,\omega)$ including vertex corrections for A_{1g} (solid line), B_{1g} (dotted line), and B_{2g} (dashed line) symmetry at $T/T_c=0.77$.

the B_{2g} response and its absence in the B_{1g} response would lend support to the current models of Fermi topology and the strength and anisotropy of the interaction.[8] In Fig. 1 for the B_{1g} response we recognize that a gap at lower ω and a pair-breaking peak at a threshold energy of $\omega=0.15t\simeq(3/2)\Delta_0$ develop as T decreases below T_c (dashed curves in Fig. 1). Here, Δ_0 is the gap amplitude of the $d_{x^2-y^2}$-wave gap which can be estimated from the binding energy at the midpoint of the leading edge in the calculated photoemission spectrum near the antinode of the gap.[14] This gap amplitude Δ_0 rises much more rapidly below T_c than the BCS d-wave gap and reaches at our lowest temperature $T=0.017t$ ($T/T_c=0.77$) a value of about $\Delta_0=0.1t$. Comparison with weak-coupling theory shows that the singularity at the pair-breaking threshold[1] is removed here by strong quasiparticle damping while according to the weak-coupling theory of Ref. 2 this singularity is removed by a screening term arising from vertex corrections due to the pairing interaction. Electron-electron scattering due to short-range Coulomb interaction can describe the observed broadening above the pair-breaking peak in the B_{1g} Raman spectrum of YBCO.[2] Recently it has been shown[14] that the collective mode due to the fluctuations of the amplitude of the d-wave gap may also yield a broadening of the calculated pair-breaking peak in Fig. 1. Our results for B_{1g} response in the superconducting state (see Fig. 1) agree qualitatively with results of non-self-consistent calculations which include the effect of inelastic scattering.[8]

The Raman response function for B_{2g} symmetry shown in Fig. 2 does not exhibit such dramatic effects below T_c as that for B_{1g} symmetry in Fig. 1. One notices that the spectrum is linear in ω for small ω and that the slope at $\omega=0$ decreases and the normal state peak broadens and shifts to somewhat higher frequency as T decreases below T_c (dashed curves in Fig. 2). The spectrum above this peak is somewhat enhanced up to frequencies near the pair-breaking threshold. In contrast to our results shown in Fig. 2 the non-self-consistent calculation yields a distinct pair-breaking peak below T_c in the B_{2g} response which occurs much closer to the B_{1g} pair-breaking peak.[8] We do not show the calculated Raman spectrum for A_{1g} symmetry because it is quite similar to that for the B_{1g} symmetry. In order to obtain the measured $A^{x'x'}$ spectrum we have to add to the A_{1g} spectrum the B_{2g} spectrum. The resulting $A^{x'x'}$ response starts linearly in ω because at low frequencies it is dominated by the B_{2g} spectrum up to a shoulder corresponding to the small peak in the B_{2g} spectrum. For higher frequencies the $A^{x'x'}$ spectrum is dominated by the A_{1g} component exhibiting the large pair-breaking peak (see Fig. 3).

We come now to the discussion of the effect of vertex corrections on the Raman response functions. From Eq. (4) one sees that the general trend of the vertex correction J is to suppress the response in the B_{1g} channel and to enhance the response in the B_{2g} channel while we have a mixed effect on the A_{1g} channel because the component of $\gamma_{A_{1g}}$ proportional to t is suppressed and the component proportional to $t'=-Bt$ is enhanced. Inserting our results for the pairing interaction P_s and the spectral functions N and A_1 into the expression for the correction J in Eq. (5) we obtain a rather large value for J. This means that our lowest order approximation of the vertex equation (3) overestimates the vertex correction. In Fig. 3 we show the different effects of the vertex correction J (multiplied by a small factor) on the three Raman response functions in the superconducting state. Comparison with Figs. 1 and 2 shows that the B_{1g} response is strongly suppressed while the B_{2g} response is slightly enhanced. The pair-breaking peak in the A_{1g} response function becomes now somewhat smaller than that in the B_{1g} response while in the absence of vertex corrections the former peak is much larger than the latter peak.

Recently, a sharp Raman resonance of B_{1g} symmetry at about 75 meV has been observed in underdoped Bi2212 compounds at different doping levels.[21] The question arises whether or not this resonance has its origin in the normal-state pseudogap which has been inferred from measurements of the specific heat and Knight shift,[15] angle-resolved photoemission (ARPES),[16] and tunneling density of states[17] in underdoped cuprates. We have shown previously that a phenomenological d-wave pseudogap $E_g(\mathbf{k})=E_g[\cos(k_x)-\cos(k_y)]$, together with the normal-state self-energy components determined by the FLEX approximation is capable of describing qualitatively the Knight shift, nuclear-spin relaxation rate $1/T_1$, ARPES, and tunneling data in the underdoped cuprates.[19] It should be stressed that this is a nontrivial calculation because the pseudogap gives rise to anomalous

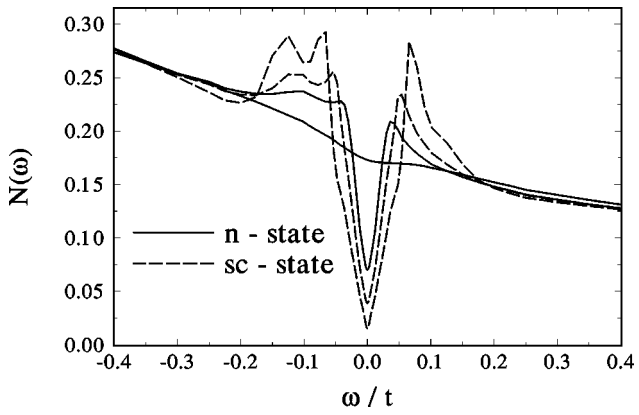

FIG. 4. Density of states $N(\omega)$ for d-wave pseudogap with amplitude $E_g=0.05t$, in the normal state at $T=0.1t$ and $0.023t$ (solid lines) and in the superconducting state at $T=0.021t$ and $0.018t$ $(T/T_c)=0.78$ (dashed lines). The values $N(0)$ decrease in this sequence of temperatures.

Green's functions contributions to the susceptibilities which in turn lead to strong effects on the quasiparticle self-energies. Below T_c the square of the total gap becomes equal to $E_g^2(\mathbf{k})+|\phi(\mathbf{k},\omega)|^2$ where ϕ is calculated self-consistently from the Eliashberg gap equation. In Fig. 4 we show our results for the density of states $N(\omega)$ for a pseudogap amplitude $E_g=0.05t$ which is assumed to be temperature independent. One sees that for decreasing T a typical d-wave gap develops also in the normal state and that this spectrum merges continuously into the superconducting spectrum as T decreases through $T_c=0.022t$. One can see that below T_c a dip develops at negative ω below the quasiparticle peak and that the spectrum is quite asymmetric with respect to the Fermi energy at $\omega=0$. These results are quite similar to the measured tunneling spectra in underdoped Bi2212 (Ref. 17) apart from the double peak at negative ω values occurring in Fig. 4 which is not seen in the experiments.

These results encourage us to calculate the Raman response functions above and below T_c in the presence of this d-wave pseudogap $E_g(\mathbf{k})$. In Fig. 5(a) we show our results for the B_{1g} symmetry again for a gap amplitude $E_g=0.05t$ as in Fig. 4. Comparison with the results for $E_g=0$ in Fig. 1 shows that the most prominent effect of the pseudogap is to produce a broad peak at about a frequency $\omega\simeq 0.075t \simeq(3/2)E_g$ as T approaches T_c from above. This frequency is nearly the same as the frequency difference between the quasiparticle peaks in the density of states in Fig. 4. We have also carried out calculations for larger values of the gap amplitude E_g corresponding to lower doping levels,[15,17] i.e., $E_g=0.075t$ and $0.1t$.[19] Then we find analogous results, namely, that for decreasing T in the normal state a peak evolves in the B_{1g} Raman spectrum at a frequency of about $(3/2)E_g$ which corresponds to the frequency difference between the peaks in the density of states. The continuous evolution of the B_{1g} Raman peak for decreasing T as shown in Fig. 5(b) for $E_g=0.15t$ is similar to the observed evolution of the peak in slightly underdoped Bi2212.[21] We note that the position of the peak at about $\omega\simeq 0.25t\simeq 62$ meV for $t=250$ meV is of the order of magnitude of the observed resonance at 75 meV.[21] The increase of the normal-state

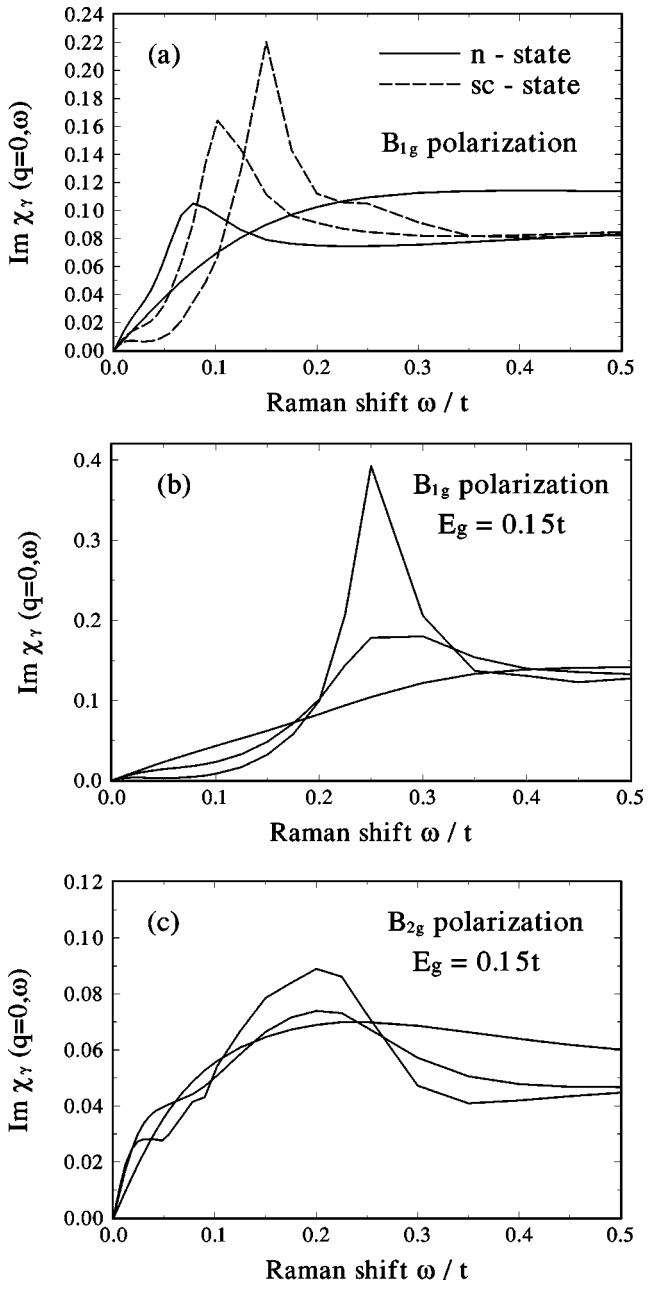

FIG. 5. (a) Raman intensity for B_{1g} polarization with d-wave pseudogap amplitude $E_g=0.05t$ in the normal state at $T=0.1t$ and $0.023t$ (solid lines with increasing slopes), and in the superconducting state at $T=0.021t$ and $0.018t$ $(T/T_c)=0.78$ (dashed lines with increasing peaks). (b) The same for $E_g=0.15t$ and $T=0.1$, 0.050, and $0.030t$ in the normal state (increasing peaks in this sequence). (c) B_{2g} Raman response for $E_g=0.15t$ and the same T as in (b) (increasing peaks in this sequence).

peak for decreasing T is accompanied by a suppression of low-frequency spectral weight as it is seen in the experiments [see Fig. 5(b)].[21]

The question arises whether the pseudogap can explain also the normal-state data for B_{2g} Raman spectra of YBCO and Bi2212 in the underdoped regime where a reduction of spectral weight for decreasing temperature is observed.[22] We find indeed that spectral weight at higher Raman shifts is lost while the slope at $\omega=0$ is increased for decreasing temperature T [see Fig. 5(c) for $E_g=0.15t$]. The broad peak arising

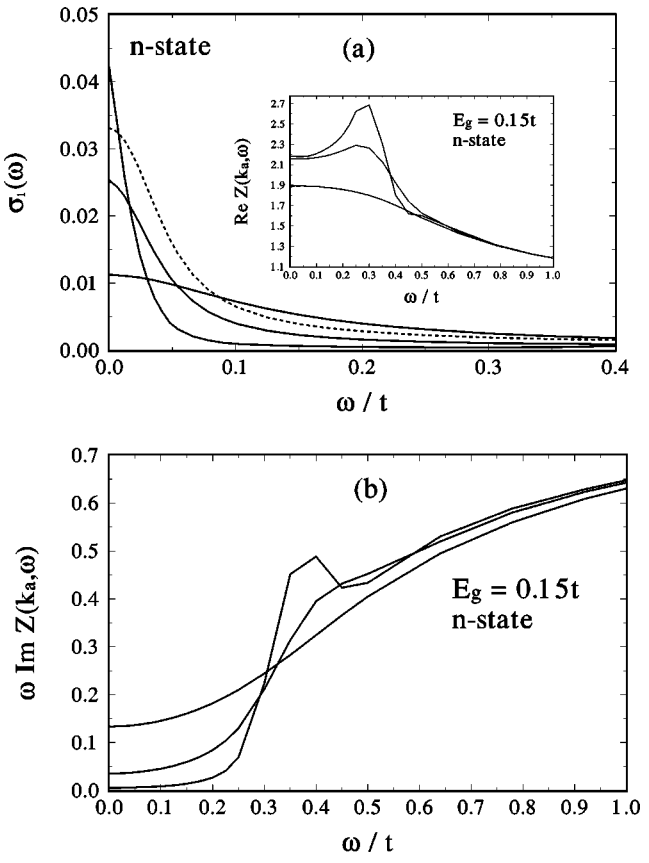

FIG. 6. (a) Optical conductivity $\sigma_1(\omega)$ for amplitude $E_g = 0.15t$ of the pseudogap, at temperatures $T = 0.1$, 0.050, and $0.030t$; inset: $\mathrm{Re}\, Z(\mathbf{k}_a, \omega)$ for the same temperatures (increasing peaks at $\omega = 0$ in this sequence); dashed line for $E_g = 0$ and $T = 0.030t$. (b) Quasiparticle damping, $\omega \mathrm{Im}\, Z(\mathbf{k}_a, \omega)$, at antinode $\mathbf{k}_a$, for amplitude $E_g = 0.15t$ of the pseudogap, at temperatures $T = 0.1$, 0.050, and $0.030t$ (decreasing values at $\omega = 0$ in this sequence of temperatures).

below the pair-breaking threshold $2E_g$ is much less pronounced than the sharp peak occurring in the B_{1g} Raman spectrum [see Fig. 5(b)]. In the superconducting state the slope at $\omega = 0$ decreases for decreasing T in agreement with the experimental data for the B_{2g} channel, however, our pair-breaking maximum (see Fig. 2) is much less pronounced than the experimental one.[22]

Finally, we discuss our normal-state results for the optical in-plane conductivity $\sigma_1(\omega)$ in the presence of a d-wave pseudogap $E_g(\mathbf{k})$. This has the form of a Drude peak where for increasing E_g the maximum at $\omega = 0$ is increased which is balanced by a loss of spectral weight at higher frequencies [see Fig. 6(a) for $E_g = 0.15t$]. The quasiparticle damping, $\Gamma(\mathbf{k}, \omega) = \omega\, \mathrm{Im}\, Z(\mathbf{k}, \omega)$ is highly anisotropic and exhibits for $\mathbf{k}$ along the direction of the antinode of the gap and for decreasing T a gap of the order E_g [see Fig. 6(b) for $E_g = 0.15t$]. At the same time the effective mass ratio $m^*/m = \mathrm{Re}\, Z(\mathbf{k}, \omega)$ is enhanced at about $\omega \simeq 2E_g$ above its value at $\omega = 0$ where $\mathrm{Re}\, Z \approx 2$ [see inset in Fig. 6(a)]. In the absence of the pseudogap the scattering rate Γ varies linearly with frequency ω as can be seen in Fig. 6(b) for higher temperatures. These results are in qualitative agreement with optical conductivity data and the frequency-dependent scattering rate and effective mass spectra obtained from the complex optical conductivity on underdoped Bi2212, YBCO, and LSCO compounds.[20] For example, for underdoped Bi2212 with $T_c = 67$ K the scattering rate $1/\tau(\omega)$ is linear in ω at $T > T^* \simeq 200$ K, and for $T < T^*$ the low-frequency scattering rate is suppressed for $\omega < 500 - 700\,\mathrm{cm}^{-1}$ (62–87 meV).[20] This is in qualitative agreement with our results shown in Fig. 6(b) from which we estimate a $T^* \simeq 0.1t \simeq 250$ K and a threshold energy for the steep rise of about $0.3t \simeq 75$ meV. It should be stressed that we have *calculated* the frequency-dependent scattering rate and mass enhancement with the help of the FLEX equations while these quantities have been obtained in Ref. 20 from theoretical expressions involving the complex conductivity.

IV. CONCLUSIONS

In summary, we have calculated the electronic Raman response function within the framework of the FLEX approximation for the 2D Hubbard model. The FLEX approximation is capable of describing the most important properties of the high-T_c cuprates, namely, their unusual normal state behavior arising from strong electronic correlations, and the unconventional superconducting state which is widely believed to have $d_{x^2-y^2}$ wave pairing. These properties are reflected in the calculated Raman response functions for A_{1g} or $A^{x'x'}$, B_{1g}, and B_{2g} polarizations. In the normal state these spectra start linearly in frequency ω with a slope that increases with decreasing temperature T, and at high frequencies these spectra become almost constant. The latter property is a consequence of the linear frequency variation of the quasiparticle damping. In the superconducting state one obtains a gap and a pair-breaking peak in the B_{1g} channel because this polarization probes the region in momentum space around the antinode of the gap. The effect of superconductivity on the B_{2g} spectrum is much smaller which is not surprising because the B_{2g} channel probes the region around the node of the gap. Our results for photoemission and Raman spectra agree qualitatively with experiments on optimally doped cuprates.

The exotic behavior of the cuprates in the underdoped regime can be described qualitatively by a phenomenological normal-state d-wave gap which enters the expressions of the FLEX approximation in addition to the superconducting gap occurring below T_c.[19] Here we show that such a pseudogap leads in the density of states for decreasing T to the development of a typical d-wave gap structure which merges continuously into the superconducting spectrum. These results are in agreement with recent STM data.[17] A corresponding pair-breaking peak develops continuously in the B_{1g} spectrum as T decreases in the normal state and below T_c. The increase of the normal-state peak is accompanied by suppression of low-frequency spectral weight for decreasing T. These results are similar to the recently observed resonance and simultaneous reduction of low-frequency intensity in the B_{1g} spectrum of underdoped Bi2212.[21] However, this interpretation is somewhat questionable because the resonance energy of 75 meV is almost independent of doping level while one needs a pseudogap whose amplitude increases with decreasing doping level in order to describe the Knight-shift and tunneling measurements.[19] This issue should be clarified experimentally.

Support for the existence of a pseudogap in the underdoped cuprates is obtained from our results for the optical conductivity and their agreement with experiment. The presence of a pseudogap leads at lower temperatures to an increase of the maximum of the Drude peak which is balanced by a loss of spectral weight at higher frequencies [see Fig. 6(a)]. At the same time a gap develops for decreasing temperature in the quasiparticle damping below a threshold frequency of the order of the pseudogap amplitude [see Fig. 6(b)]. These results are in qualitative agreement with the in-plane optical conductivity data in underdoped cuprates.[20] This makes us believe that the calculated peaks in the Raman spectra should be observable in the underdoped cuprates as well.

ACKNOWLEDGMENTS

We acknowledge helpful discussions with D. Fay and K. Scharnberg. D.M. acknowledges financial support by the Deutsche Forschungsgemeinschaft via the Graduiertenkolleg ''Physik nanostrukturierter Festkörper.''

APPENDIX: VERTEX FUNCTION AND WARD'S IDENTITY

First we show that Ward's identity for the electromagnetic kernel holds also for the FLEX approximation. The general expression of the current-charge correlation function in the 2×2 Nambu matrix formalism is given by[23]

$$P_{\mu\nu}=-e^2\sum_k \frac{1}{2}\mathrm{Tr}[\gamma_\mu(k,k+q)G(k+q)\Gamma_\nu(k+q,k)G(k)];$$
$$(\mu,\nu=1,2,3,0), \tag{A1}$$

with

$$q\equiv\mathbf{q},i\nu_m, \quad k\equiv\mathbf{k},i\omega_n, \quad \sum_k = T\sum_{i\omega_n}\sum_{\mathbf{k}}.$$

Here, Γ_ν is the dressed vertex function, and γ_μ is the bare current-charge vertex

$$\gamma_\mu(k,k+q)=v_\mu(\mathbf{k}+\mathbf{q}/2)\tau_0 \quad (\mu=1,2,3),$$
$$\gamma_0=\tau_3. \tag{A2}$$

Notice that $P_{00}(q)=e^2\chi_{c0}(q)$ where χ_{c0} is the irreducible charge susceptibility.[12] The Dyson equation yields the dressed 2×2 matrix Green's function G in terms of the bare Green's function G_0 and the self-energy Σ

$$G^{-1}(k)=G_0^{-1}(k)-\Sigma(k)$$
$$=i\omega_n Z(k)\tau_0-[\epsilon(k)+\xi(k)]\tau_3-\phi(k)\tau_1. \tag{A3}$$

In the FLEX approximation for the Hubbard Hamiltonian the self-energy Σ is determined by the following generalized Eliashberg equations[10]:

$$\Sigma(k)=\sum_{k'}[P_s(k-k')\tau_0 G(k')\tau_0+P_c(k-k')\tau_3 G(k')\tau_3],$$

with

$$P_s(q)=(3/2)U^2\chi_s(q), \quad \chi_s=\chi_{s0}(1-U\chi_{s0})^{-1},$$
$$P_c(q)=(1/2)U^2\chi_c(q), \quad \chi_c=\chi_{c0}(1+U\chi_{c0})^{-1}. \tag{A4}$$

The ladder approximation for the vertex function Γ_μ corresponding to the FLEX approximation for Σ yields the following linear equation:

$$\Gamma_\mu(k+q,k)=\gamma_\mu(k+q,k)$$
$$+\sum_{k'}[\tau_0 G(k'+q)\Gamma_\mu(k'+q,k')G(k')$$
$$\times\tau_0 P_s(k-k')+\tau_3 G(k'+q)\Gamma_\mu(k'+q,k')$$
$$\times G(k')\tau_3 P_c(k-k')]. \tag{A5}$$

We note that the equation for Γ_0 is identical to the vertex equation for the irreducible charge susceptibility χ_{c0} in Eq. (6) of Ref. 12.

Gauge invariance of the electromagnetic kernel requires that Γ_μ satisfies the Ward identity[23]

$$\sum_\mu q_\mu\Gamma_\mu(k+q,k)=\tau_3 G^{-1}(k)-G^{-1}(k+q)\tau_3. \tag{A6}$$

One can derive Ward's identity (A6) from Eq. (A5) by inserting Eq. (A6) on the right side in the resulting equation and then making use of the Eliashberg equation (A4). For $\mathbf{q}=0$ it follows from Eq. (A6) the important relationship $P_{00}(\mathbf{q}=0,i\nu_m)=e^2\chi_{c0}(\mathbf{q}=0,i\nu_m)=0$. Furthermore, we obtain from Ward's identity in Eq. (A6) for $\mathbf{q}=0$ the following expression for the vertex Γ_0:

$$\Gamma_0(\mathbf{k},\omega+\nu,\omega)=Z(\mathbf{k},\omega+\nu)\tau_3$$
$$+\omega[Z(\mathbf{k},\omega+\nu)-Z(\mathbf{k},\omega)]\nu^{-1}\tau_3$$
$$-[\xi(\mathbf{k},\omega+\nu)-\xi(\mathbf{k},\omega)]\nu^{-1}\tau_0$$
$$+[\phi(\mathbf{k},\omega+\nu)+\phi(\mathbf{k},\omega)]\nu^{-1}\tau_3\tau_1. \tag{A7}$$

The last term proportional to $\tau_3\tau_1=i\tau_2$ in Eq. (A7) diverges for $\nu\to 0$ and corresponds to the collective gauge mode.[23,14] This is renormalized by the Coulomb interaction to the 2D plasmon.

We turn now to the Raman response function χ_γ for polarization symmetry γ [see Eq. (2)]. This is derived from $P_{00}(q)$ in Eq. (A1) by replacing γ_0 and Γ_0 by the bare and full Raman vertices $\gamma\tau_3$ and $\Gamma\tau_3$:

$$\chi_\gamma(Q)=-\sum_k \frac{1}{2}\mathrm{Tr}[\Gamma(k+Q,k)\tau_3 G(k+Q)\gamma(\mathbf{k})\tau_3 G(k)]. \tag{A8}$$

The full Raman vertex Γ satisfies the following integral equation:

$$\Gamma(k+Q,k)=\gamma(\mathbf{k})+\sum_q [P_s(q)+P_c(q)] \times\frac{1}{2}\mathrm{Tr}[\tau_3 G(k+q+Q)\tau_3 G(k+q)] \times\Gamma(k+q+Q,k+q). \quad \text{(A9)}$$

Relabeling of variables and analytical continuation in Eqs. (A8) and (A9) from $Q\equiv\mathbf{Q},i\nu_m$ to $\mathbf{Q}=0,\omega$, $k\equiv\mathbf{k},i\omega_n$ to $\mathbf{k},\omega'$, and $q\equiv\mathbf{q},i\mu_m$ to $\mathbf{q},\nu$, leads to Eqs. (1) and (3).

We redefine now the vertex function Γ by $\Lambda(k+Q,k)\equiv\Gamma(k+Q,k)/\gamma(\mathbf{k})$. The resulting equation (A9) for Λ contains on the right hand side under the integral over $\mathbf{q}$ the factor $\gamma(\mathbf{k}+\mathbf{q})/\gamma(\mathbf{k})$. Since $P_s(q)$ is strongly peaked at $\mathbf{\Pi}=(\pi,\pi)$ and since for B_{2g} (B_{1g}) Raman polarization $\gamma_{B_{2g}}(\mathbf{k}+\mathbf{\Pi})=\gamma_{B_{2g}}(\mathbf{k})$ [$\gamma_{B_{1g}}(\mathbf{k}+\mathbf{\Pi})=-\gamma_{B_{1g}}(\mathbf{k})$] [see Eq. (2)], we can approximately set

$$\gamma_{B_{2g}}(\mathbf{k}+\mathbf{q})/\gamma_{B_{2g}}(\mathbf{k})\simeq+1,$$
$$\gamma_{B_{1g}}(\mathbf{k}+\mathbf{q})/\gamma_{B_{1g}}(\mathbf{k})\simeq-1. \quad \text{(A10)}$$

Then the equation for the vertex function $\Lambda_{B_{2g}}$ agrees with Eq. (A5) for the vertex Γ_0 of the charge density. This is given for $\mathbf{q}=0$ by Eq. (A7). Ignoring the collective mode term and letting ν tend to zero we estimate that

$$\Gamma_{B_{2g}}(\mathbf{k},\omega',\omega)\simeq\gamma_{B_{2g}}(\mathbf{k})[Z(\mathbf{k},\omega')+\omega'(d/d\omega')Z(\mathbf{k},\omega')]. \quad \text{(A11)}$$

*Present address: Freie Universität Berlin, Fachbereich Physik, Institut für Theoretische Physik, Arnimallee 14, D-14195 Berlin, Germany.

[1] T. P. Devereaux *et al.*, Phys. Rev. Lett. **72**, 396 (1994); T. P. Devereaux and D. Einzel, Phys. Rev. B **51**, 16 336 (1995); **54**, 15 547 (1996); D. Einzel and R. Hackl, J. Raman Spectrosc. **27**, 307 (1996).
[2] D. Manske, C. T. Rieck, R. Das Sharma, A. Bock, and D. Fay, Phys. Rev. B **56**, R2940 (1997).
[3] C. M. Varma *et al.*, Phys. Rev. Lett. **63**, 1996 (1989); **64**, 497 (1990).
[4] J. Ruvalds, Supercond. Sci. Technol. **9**, 905 (1997).
[5] P. Monthoux and D. Pines, Phys. Rev. B **50**, 16 015 (1994).
[6] D. Branch and J. P. Carbotte, Phys. Rev. B **54**, 13 288 (1996).
[7] T. P. Devereaux and A. Kampf, Phys. Rev. B **59**, 6411 (1999).
[8] A. Bille, C. T. Rieck, and K. Scharnberg, in *Symmetry and Pairing in Superconductors*, edited by M. Ausloos and S. Kruchinin (Kluwer, Dordrecht, 1999).
[9] N. E. Bickers, D. J. Scalapino, and S. R. White, Phys. Rev. Lett. **62**, 961 (1989); N. E. Bickers and D. J. Scalapino, Ann. Phys. (N.Y.) **193**, 206 (1989).
[10] T. Dahm and L. Tewordt, Phys. Rev. Lett. **74**, 793 (1995); Phys. Rev. B **52**, 1297 (1995); Physica C **246**, 61 (1995); T. Dahm, Solid State Commun. **101**, 487 (1997).
[11] G. Baym and L. P. Kadanoff, Phys. Rev. **124**, 287 (1961); G. Baym, *ibid.* **127**, 1391 (1962).
[12] S. Wembter and L. Tewordt, Physica C **199**, 375 (1992).
[13] T. Dahm and L. Tewordt, Physica C **265**, 67 (1996).
[14] T. Dahm, D. Manske, and L. Tewordt, Phys. Rev. B **58**, 12 454 (1998).
[15] G. V. M. Williams *et al.*, Phys. Rev. Lett. **78**, 721 (1997); Phys. Rev. B **58**, 15 053 (1998).
[16] D. S. Marshall *et al.*, Phys. Rev. Lett. **76**, 4841 (1996); J. M. Harris *et al.*, Phys. Rev. B **54**, R15665 (1996).
[17] Ch. Renner *et al.*, Phys. Rev. Lett. **80**, 149 (1998).
[18] T. Dahm, D. Manske, and L. Tewordt, Phys. Rev. B **55**, 15 274 (1997).
[19] T. Dahm, D. Manske, and L. Tewordt, Phys. Rev. B **56**, R11 419 (1997); J. Low Temp. Phys. **111**, 879 (1998).
[20] A. V. Puchkov, D. N. Basov, and T. Timusk, J. Phys.: Condens. Matter **8**, 10 049 (1996); T. Startseva *et al.*, Phys. Rev. B **59**, 7184 (1999).
[21] G. Blumberg *et al.*, Science **278**, 1427 (1997); J. Phys. Chem. Solids **59**, 1932 (1998).
[22] R. Nemetschek *et al.*, Phys. Rev. Lett. **78**, 4837 (1997).
[23] J. R. Schrieffer, *Theory of Superconductivity* (Addison-Wesley, Redwood City, CA, 1964).